Regulation of the Rate and Extent of Phospholipase C β_2 Effector Activation by the $\beta\gamma$ Subunits of Heterotrimeric G Proteins†

Loren W. Runnels‡ and Suzanne F. Scarlata*

Department of Physiology & Biophysics, State University of New York at Stony Brook, Stony Brook, New York 11794-8661

Received May 14, 1998; Revised Manuscript Received July 17, 1998

ABSTRACT: The activity of mammalian phosphoinositide-specific phospholipase C β_2 (PLC-β_2) is regulated by the α_q family of G proteins and by $\beta\gamma$ subunits. We measured the affinity between the laterally associating PLC-β_2 and G$\beta\gamma$ on membrane surfaces by fluorescence resonance energy transfer. Using a simple model, we translated this apparent affinity to a bulk or three-dimensional equilibrium constant (K_d) and obtained a value of 3.2 μM. We confirmed this K_d by separately measuring the on and off (k_f and k_r) rate constants. The k_f was slower than a diffusion-limited value, suggesting that conformational changes occur when the two proteins interact. The off rate shows that the PLC-β_2·G$\beta\gamma$ complexes are long-lived (∼123 s) and that activation of PLC-β_2 by G$\beta\gamma$ would be sustained without a deactivating factor. The addition of α_{i1}(GDP) subunits failed to physically dissociate the complex as determined by fluorescence. However, enzyme activity studies performed under similar conditions show that the addition of Gα_{i1}(GDP) results in reversal of PLC-β_2 activation by G$\beta\gamma$ during the time of the assay (30 s). From these results, we propose that Gα(GDP) subunits can bind to the PLC-β_2·G$\beta\gamma$ complex to allow for rapid deactivation without complex dissociation. In support of this model, we show by fluorescence that Gα_{i1}(GDP)·G$\beta\gamma$·PLC-β_2 can form.

Heterotrimeric guanine nucleotide-binding proteins or G proteins, composed of α, β, and γ subunits, play a major role in the transduction of extracellular signals to the inside of cells. Signaling through G proteins initially occurs by the extracellular binding of an agonist to its specific seven-transmembrane receptor, resulting in receptor activation. The activated receptor in turn catalyzes the exchange of GDP for GTP on the α subunit on the inner surface of the plasma membrane. This exchange induces allosteric changes in the α subunit that lower its affinity for $\beta\gamma$ subunits. Gα(GTP) and G$\beta\gamma$ are then thought to dissociate on the membrane surface, allowing them to either activate or inhibit signaling pathways by directly regulating the activities of effectors such as adenylyl cyclases, ion channels, and phospholipases (for reviews see refs *1*−*5*). The duration of the signal generated by the Gα(GTP)·effector interaction is regulated by GTPase activity on the α subunit. Hydrolysis of GTP to GDP lowers the affinity of α subunits for effectors and raises its affinity for $\beta\gamma$ subunits. The lifetime of the Gα-generated signal is thus dependent on its intrinsic rate of GTP hydrolysis and can be accelerated by the binding of GTPase-activating proteins or GAPs (see refs *6* and *7* for background).

Unlike α subunits, cessation of G$\beta\gamma$·effector signaling does not have an analogous deactivation switch but is thought to be primarily mediated by the reassociation of G$\beta\gamma$ with Gα(GDP). Reassociation could occur by either concerted displacement of the G$\beta\gamma$ subunits from effectors by Gα(GDP), or by Gα(GDP) binding to free G$\beta\gamma$ following G$\beta\gamma$· effector dissociation. The rate of deactivation of G$\beta\gamma$ signaling would then depend on at least three variables: the relative G$\beta\gamma$ affinities for its effectors and for Gα(GDP), the local concentration of free Gα(GDP) and G$\beta\gamma$ effectors, and the intrinsic rate of dissociation of G$\beta\gamma$ from effector molecules. It has been proposed that, by stimulating Gα-GTPase catalytic activity, GAPs could regulate G$\beta\gamma$ signaling by temporally controlling the concentration of Gα(GDP) (*7*). In support, recent work has shown that a newly discovered family of GAPs proteins known as regulators of G protein signaling or RGS proteins can control the rapid gating kinetics of $\beta\gamma$-activated inwardly rectifying K^+ channels (*8*). However, little is known about the physical interactions between G$\beta\gamma$ and effector(s) that regulate the lifetime of G$\beta\gamma$-mediated signaling. Indeed, sequestering of G$\beta\gamma$ subunits from other interacting species, such as the complementary Gα subunits and other effectors, could influence the response time and possibly the pathway of cell signaling.

In this paper, we have characterized the interaction between G$\beta\gamma$ subunits and the β class of phosphoinositide-specific phospholipase C (PLC-β)[1] effectors. PLC-β is a member of a family of closely related mammalian phosphoinositide-specific phospholipase (PI-PLCs) enzymes, PI-PLC-β, PI-PLC-γ, and PI-PLC-δ, that associate with membranes to carry out hydrolysis of phosphoinositide substrates. In eukaryotic cells, the principal activity of PI-PLCs is to catalyze the hydrolysis of phosphatidylinositol 4,5-bisphosphate [PtdIns(4,5)P_2] to generate two second messengers,

† This work was supported by the National Institutes of Health GM43124.

* Corresponding author: Phone 516-444-3071; FAX 516-444-3432; e-mail suzanne@physiology.pnb.sunysb.edu.

‡ Present address: Children's Hospital/HHMI, Department of Cardiology Research, Enders 1309, P.O. Box EN-306; 320 Longwood Ave., Boston, MA 02115.

10.1021/bi9811258 CCC: $15.00
Published on Web 10/07/1998

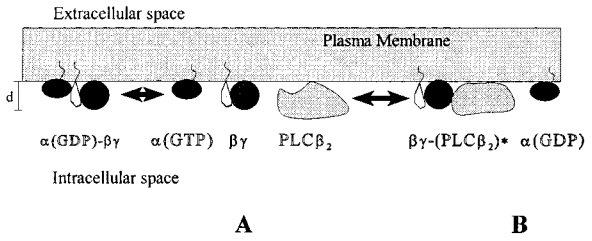

FIGURE 1: Cartoon of the interactions addressed in this study. In (A) the inactive α(GDP)·$\beta\gamma$ dissociates due to the replacement of GTP for GDP on the α subunit. The $\beta\gamma$ subunit can then interact with an effector such as PLC-β_2 to form an activated complex in the plane of the membrane as denoted by a change in conformation (B). Deactivated (i.e., GDP-bound) α subunits can diffuse laterally and possibly rebind G$\beta\gamma$ subunits. In this study, we will work under conditions where all of the components are membrane-bound and the proteins can interact within a surface volume, v, which is proportional to the outer radius of the vesicle, and the thickness of the interface in which the proteins can interact is estimated by the approximate diameter (d) of the proteins (see eq 1).

diacylglycerol (DAG) and inositol 1,4,5-trisphosphate (Ins-[1,4,5)P_3], which mediate the activation of protein kinase C and intracellular Ca^{2+} ion release, respectively (for reviews see refs *9* and *10*). PLC-β enzymes are regulated by the G_q family of heterotrimeric G proteins; many isoforms of G$\beta\gamma$ subunits can also directly stimulate PLC-β enzymatic activity in vitro and the PLC-β_2 isoforms are responsive to G$\beta\gamma$ stimulation (*11*−*14*).

To date, little is known about the interactions between G proteins and their effectors since few techniques allow for direct observation of associations of membrane-bound proteins. Here, we have used fluorescence spectroscopy of the purified proteins bound to lipid bilayers (*15*; Materials and Methods) to investigate the energy and time of association of G$\beta\gamma$ with PLC-β_2 effectors and how these parameters are influenced by Gα subunits. A cartoon depicting these associations is shown in Figure 1. We find that although the lifetime of the G$\beta\gamma$·PLC-β_2 complex is long ($\tau \sim 123$ s), reversal of PLC-β_2 activation by Gα(GDP) can occur rapidly. Our experiments support a model in which this rapid deactivation of G$\beta\gamma$·PLC-β_2 by Gα(GDP) occurs through the formation of a transient ternary complex [Gα(GDP)·G$\beta\gamma$·PLC-β_2].

MATERIALS AND METHODS

Materials. The purification of recombinant PLC-β_2 has been described (*15*). G protein $\beta\gamma$ subunits were purified from cholate detergent extracts of bovine brain membranes using the method of Sternweis and Robishaw, substituting octyl-Sepharose (Pharmacia) for the final step (*16*). The proteins were further purified to separate any contaminating G protein α subunits by activating the pooled fractions with AMF (20 μM $AlCl_3$, 10 mM $MgCl_2$, 10 mM NaF, 10 μM GDP), diluting in half with buffer A (20 mM Hepes, 50 mM NaCl, 5 mM KH_2PO_4, pH 8.0, 1 mM DTT, and 1% octyl glucoside), applying to a 3 mL Bio-Gel hydroxyapatite (Bio-Rad) column, and eluting with a 40 mL gradient of 5−300 mM KH_2PO_4 in buffer A supplemented with AMF. Fractions containing G protein $\beta\gamma$ subunits purified to apparent homogeneity, as determined by SDS−PAGE and Coomassie staining, were pooled and diluted into buffer A 4-fold and then reapplied to the 3 mL Bio-Gel HPHT (Bio-Rad) column. To further concentrate the G protein $\beta\gamma$ subunits, bound protein was eluted with isocratic application of buffer A supplemented with 150 mM KH_2PO_4, collecting 0.5 mL fractions.

$G\alpha_{i1}$ (pQE-6-Giα_1) was cotransformed with *Saccharomyces cerevisiae* protein *N*-myristoyltransferase (pNMT) in JM109 cells, expressed, and purified using the procedure of Lee et al. (*17*), substituting a Q2 column (Bio-Rad) for Q-Sepharose and Source 15 Phenyl (Pharmacia) for phenyl-Superose resin.

The G$\alpha_o\beta\gamma$ heterotrimer was purified from cholate detergent extracts of bovine brain membranes using the method of Sternweis and Robishaw with the following modifications (*16*). Following size-exclusion chromatography, pooled fractions containing the G$\alpha_o\beta\gamma$ heterotrimer were kept inactivated, diluted to 0.25% cholate and 300 mM NaCl, and applied to a 50 mL octyl-Sepharose column. The column was washed with one column volume of buffer B (20 mM Tris, pH 8.0, 300 mM NaCl, 0.25% cholate, and 30 mM 2-mercaptoethanol), and protein was eluted with a double reverse gradient over three column volumes from 100% buffer B to 100% buffer C (20 mM Tris, pH 8.0, 50 mM NaCl, 1.2% cholate, and 30 mM 2-mercaptoethanol), collecting 5 mL fractions. The proteins were further purified by diluting into buffer D (20 mM Hepes, 50 mM NaCl, 5 mM KH_2PO_4, pH 8.0, 30 mM 2-mercaptoethanol, and 0.7% CHAPS), applying to a 3 mL Bio-Gel hydroxyapatite (Bio-Rad) column, and eluting with a 40 mL gradient of 5−300 mM KH_2PO_4 in buffer D, collecting 1 mL fractions. Fractions containing G$\alpha_o\beta\gamma$ heterotrimer were purified to apparent homogeneity, as determined by SDS−PAGE and Coomassie staining. The identity and purity of all proteins were assessed by western blotting following SDS−PAGE. After purification samples were aliquoted, frozen in liquid nitrogen, and stored at −80 °C.

Preparation of Lipid Vesicles. 1-Palmitoyl-2-oleoyl-*sn*-glycero-3-phosphocholine (PC), 1-palmitoyl-2-oleoyl-*sn*-glycero-3-phosphoethanolamine (PE), and 1-palmitoyl-2-oleoyl-*sn*-glycero-3-[phospho-L-serine] (PS) were purchased from Avanti Polar Lipids, Inc. (Alabaster, AL). [H^3]PtdIns-(4,5)P_2 from [^{3}H]-*myo*-inositol-fed turkey erythrocyte source and PtdIns(4,5)P_2 from type I Folch fraction source (Sigma, St. Louis, MI) were a generous gift from Dr. Andrew Morris (SUNY Stony Brook, Stony Brook, NY). Lipid bilayers were prepared by extrusion, using the method of Hope et al. (*18*) to produce uniform large unilamellar vesicles (LUVs) of 100 nm diameter. Sucrose-loaded vesicles (SLVs) were prepared by the method described by Cifuentes et al. (*19*). Lipid concentrations were determined by phosphate analysis (*20*).

PLC Activity Assays. PLC activity was determined by either reconstituting the enzyme with 1 mM extruded phospholipid vesicles composed of a mixture of 1:1:1 PC:

[1] Abbreviations: PLC, phosphoinositol-specific phospholipase C; PtdIns(4,5)P_2, phosphatidylinositol 4,5-bisphosphate; DAG, diacylglycerol; Ins(1,4,5)P_3, inositol 1,4,5-triphosphate; A, 6-acryloyl-2-(dimethylamino)naphthalene (acrylodan); C, 7-diethylamino-3-(4′-maleimidylphenyl)-4-methylcoumarin; DABMI, 4-(dimethylamino)-phenylazophenyl-4′-maleimide; Dabcyl SE, 4-((4-(dimethylamino)-phenyl)azo)benzoic acid, succinimidyl ester; BODIPY, 8-bromomethyl-4,4-difluoro-1,3,5,7-tetramethyl-4-bora-3a,4a-diaza-s-indacene, methyl bromide); DABCYL chloride, 4-(dimethylamino)azobenzene-4′-sulfonyl chloride.

PS:PE with 2 mol % PtdIns(4,5)P_2 or with 133 μM 1:4 PtdIns(4,5)P_2:PE sonicated vesicles as described (*15*). Vesicles were doped with approximately 8000 cpm/sample [^{3}H]-PtdIns(4,5)P_2 (New England Nuclear) to follow the PLC-catalyzed hydrolysis of PtdIns(4,5)P_2. The following protocol was used for the 30 s time course of Gα_{i1} deactivation of G$\beta\gamma$·PLC-β_2 activity study. Samples containing vesicle substrate, G$\beta\gamma$, and PLC-β_2 are incubated at 37 °C for 5 min to allow the sample temperature to thermally equilibrate and G$\beta\gamma$ sufficient time to complex with PLC-β_2. The sample initially contains 20 μL of 400 μM 1:4 PtdIns(4,5)-P_2:PE sonicated vesicle substrate in MAIN buffer (20 mM Hepes, 160 mM KCl, 3 mM EGTA, and 1 mM DTT), 10 μL of G$\beta\gamma$ or 10 μL of G$\beta\gamma$ buffer (20 mM Hepes, pH 8.0, 100 mM KCl, 30 mM 2-mercaptoethanol, and 0.7% CHAPS), and PLC-β_2 diluted into MAIN buffer with 0.5 mg/mL BSA to give a final PLC-β_2 concentration of 25−100 nM. Reactions are initiated at 37 °C with the addition of 15 μL of a 37 °C mixture of either boiled Gα_{i1} (5 μL) in buffer G (20 mM Tris, pH 8.0, and 200 mM NaCl) and MAIN plus 10 mM $CaCl_2$ (10 μL) or nonboiled Gα_{i1} (5 μL) and MAIN plus 10 mM $CaCl_2$ (10 μL), followed by vigorous mixing. Reactions are terminated 30 s after the reaction is initiated by adding sequentially 200 μL of ice-cold 10% TCA and 100 μL of 2% BSA. Samples were then incubated on ice for 5 min and subjected to centrifugation at 6600*g* for 6 min, and 300 μL of the resultant supernatant containing liberated [^{3}H]Ins(1,4,5)P_3 was subjected to scintillation counting.

Fluorescent Labeling of Phospholipase C b Isozymes. 7-Diethylamino-3-(4′-maleimidylphenyl)-4-methylcoumarin (C), 4-(dimethylamino)phenylazophenyl-4′-maleimide (DABMI), 6-acryloyl-2-(dimethylamino)naphthalene (acrylodan), 4-[[4-(dimethylamino)phenyl]azo]benzoic acid, succinimidyl ester (Dabcyl SE), 8-bromomethyl-4,4-difluoro-1,3,5,7-tetramethyl-4-bora-3a,4a-diaza-s-indacene (BODIPY 493/503 methyl bromide), and 4-(dimethylamino)azobenzene-4′-sulfonyl chloride (dabsyl chloride) were purchased from Molecular Probes (Eugene, OR).

Phospholipase C β isozymes were labeled with BODIPY 493/503 methyl bromide, Dabcyl SE, or DABMI by adding the probe from a concentrated DMF solution at a 4:1 to 3:1 probe:protein ratio on ice for 1 h in the final column buffer from its purification (25 mM Hepes, pH 7.5, 5 mM EDTA, and 5 mM EGTA). Reactions were terminated by the addition of 30 mM β-mercaptoethanol. Excess probe was removed by dialysis using Slide-A-Lyzer 10 000 MWCO, 0.1−0.5 mL cassette (Pierce Chemical Co., Rockford, IL) at 4 °C for 2 h, overnight (∼12 h), and with a final dialysis buffer change to buffer supplemented with 1 mM DTT. Phospholipase C-β isozymes were typically modified by this reaction with a labeling ratio of 2−3 mol of DABMI probes/mol of enzyme.

G protein $\beta\gamma$ subunits were labeled with either acrylodan (A), coumarin (C), or DABMI at a 2:1 probe:protein ratio for 2 h on ice. Reactions were terminated by the addition of 30 mM β-mercaptoethanol, and excess probe was removed by dialysis against 20 mM Hepes, pH 7.0, 160 mM KCl, 1% octyl glucoside, and 1 mM DTT at 4 °C.

The concentration of the labeled proteins was determined by BCA (Pierce) analysis. Afterward, the labeled proteins were aliquoted, flash-frozen with liquid nitrogen, and stored at −70 °C until further use.

It is important to note that both PLC-β_2 and G$\beta\gamma$ are large proteins (134 and 42 kDa, respectively) and there are many possible sites for thiol and amine modification. We did not investigate the position of these sites. We do note that mild thiol or amine modification of PLC-β_2 or G$\beta\gamma$ does not interfere with PLC activity or PLC activation by isolated subunits of heterotrimeric G proteins, as reported (*15*, *21*).

Fluorescence Measurements: Fluorescent lifetimes were measured at the U9B beamline of the National Synchrotron Light Source using the apparatus described (*22*). Multi-wavelength and time-resolved fluorescence data were analyzed using UTHSCSA ImageTool and in-house software (*22*).

Steady-state measurements were taken on an ISS K2 (Champaign, IL) time-resolved spectrofluorometer using a 3 mm × 3 mm × 40 mm quartz microcell (NSG Precision Cells Inc., Farmingdale, NY). Kinetic measurements were taken either on the ISS K2 or on a SLM-Aminco spectrofluorometer with a stopped-flow attachment (Milliflow SLM-Aminco, Rochester, NY). Data were corrected for light scattering of the vesicles when the contribution exceeded 1% of the emission signal, which was the case when the coumarin and BODIPY probes were used. For acrylodan, where the scattering contribution sometimes exceeded 1% of the initial signal, emission data were corrected by background subtraction using a solution of vesicles at identical concentrations.

Analysis of Affinities and Lifetimes of Protein Complexes on Membrane Surfaces. As depicted in Figure 1, we are measuring the two-dimensional association of membrane-bound proteins, and the analysis of these interactions must take into account that these associations occur on a given unit area rather than a unit volume. There have been many excellent reports on methods to study the interactions of membrane-bound proteins (e.g., *23*, *24*). One method is to express the protein concentration in terms of mole fraction present on the membrane surface (see ref *25*) thus keeping the association parameters in two-dimensional terms. Another approach (see ref *26*) uses the idea that the effective concentration of proteins bound to membranes is higher than bulk since associations that occur in three dimensions are reduced to associations on a two-dimensional surface. The effective higher concentrations can be entered into the traditional three-dimensional or bulk phase affinity and rate equations. Our approach is to derive a simple relationship between the bulk phase and membrane phase protein concentrations that will allow us to translate the apparent K_d values determined on membrane surfaces to the more familiar bulk phase ones.

We assume that the proteins interact within a surface phase of volume (υ), which is equal to the surface area of the bilayer with an outer radius r multiplied by the thickness of the membrane/solvent interface *(d)* where d is equal to the diameter of the protein (∼50 nm for G$\beta\gamma$ or PLC-β) (see Figure 1).

$$\upsilon = 4\pi r^2 d \tag{1}$$

The relationship between the bulk phase concentration of the protein, [P_b], and the membrane surface concentration, [P_m], is simply the ratio to the volume of the bulk phase solution *(V_b)* to the surface phase volume as expressed in eq 1:

$$[P_m] = (V_b/v)[P_b] = \epsilon[P_b] \quad (2)$$

This relationship in membrane and bulk concentrations allows us to relate the value of K_d of PLC-β−G$\beta\gamma$ formed on the membrane surface and the K_d for this reaction in the bulk phase.

For bulk phase equilibria the association between PLC-β_2 and G$\beta\gamma$ can be treated as follows:

$$[\text{PLC-}\beta] + [G\beta\gamma] \underset{k_r}{\overset{k_f}{\rightleftharpoons}} [\text{PLC-}\beta\cdot G\beta\gamma]$$

$$K_d = \frac{[G\beta\gamma][\text{PLC-}\beta]}{[G\beta\gamma\cdot\text{PLC-}\beta]} \quad (3)$$

The material balance for G$\beta\gamma$ is $[G\beta\gamma] + [G\beta\gamma\cdot\text{PLC-}\beta] =$ constant $= [G\beta\gamma]_o$, and that for PLC-β is $[\text{PLC-}\beta] + [G\beta\gamma\cdot\text{PLC-}\beta] =$ constant $= [\text{PLC-}\beta]_o$, where the subscript **o** denotes the total concentration of the particular species. The degree of association (α) of PLC-β with G$\beta\gamma$ can be described analytically:

$$\alpha = \frac{1}{2}(x + b) - \frac{1}{2}\sqrt{x^2 + 2x(b-2) + b^2}$$

$$\alpha \equiv \frac{[G\beta\gamma\cdot\text{PLC-}\beta]}{[G\beta\gamma]_o} x = \frac{[\text{PLC-}\beta]_o}{[G\beta\gamma]_o} b = 1 + \frac{K_d}{[G\beta\gamma]_o} \quad (4)$$

and

$$K_d = [G\beta\gamma]_o \frac{(x-\alpha)(1-\alpha)}{\alpha} \quad (5)$$

Equations 3 and 4 are applicable for proteins associating in the bulk phase.

When G$\beta\gamma$ and PLC-β_2 are confined to the membrane, their membrane concentrations (designated by the subscript m) are related to their bulk concentrations by the volume ratio (ϵ) as defined in eq 2:

$$[\text{PLC-}\beta]_{om} = \epsilon[\text{PLC-}\beta]_o \qquad [G\beta\gamma]_{om} = \epsilon[G\beta\gamma]_o$$

$$\epsilon = \frac{V_b}{v} \quad (6)$$

Inserting these relations into the expressions for K_d and α gives

$$K_{dm} = \epsilon[G\beta\gamma]_o \frac{(x-\alpha)(1-\alpha)}{\alpha} \quad (7)$$

Thus, the dissociation constant of two proteins on the membrane surface (K_{dm}) is related to the dissociation constant in the bulk solution by the factor ϵ, which relates the surface phase volume to the bulk volume.

For proteins reconstituted into large, unilamellar vesicles, ϵ can be calculated from the amount of lipid used (moles per liter):

$$\epsilon = \frac{2 \times 10^{24}}{[\text{lipid}] N_A d_\rho} \quad (8)$$

where N_A is Avogadro's number, d is the width of the surface phase (in nanometers), and ρ is the average surface area of a lipid headgroup (in square nanometer). For a lipid concentration of 350×10^{-6} M, $d = 100$ nm, and $\rho = 0.75$ nm^2, $\epsilon = 135$ (see ref *27*).

Kinetic Measurements. The association of PLC-β_2 with G protein $\beta\gamma$ subunits reconstituted into PC:PS:PE LUVs was measured under second-order conditions. PLC-β_2 was labeled with DABMI (D−PLC-β_2), and G protein $\beta\gamma$ subunits were labeled with C (C−$\beta\gamma$). The formation of the complex was followed by the change in fluorescence due to fluorescence resonance energy transfer (FRET) upon association, using a SLM-Aminco spectrofluorometer with a stopped-flow attachment (Milliflow SLM-Aminco, Rochester, NY), or an ISS K2 time-resolved spectrofluorometer.

In the high concentration range used, the equilibrium is almost completely on the side of the complex (PLC-β_2·G$\beta\gamma$), and the forward rate (k_f) can be determined without the use of the dissociation rate (k_r) (*28*). Data were thus analyzed according to a simple pseudo-first-order bimolecular reaction scheme (*29*):

$$[\text{PLC-}\beta_2] + [G\beta\gamma] \underset{k_r \cong 0}{\overset{k_f}{\rightleftharpoons}} [\text{PLC-}\beta_2\cdot G\beta\gamma] \qquad K_d = k_r/k_f \quad (9)$$

The analytical solution for second-order conditions, where $[\text{PLC-}\beta_2]_o = [G\beta\gamma]_o = P_o$, and the degree of saturation (α) is defined as $\alpha = [\text{PLC-}\beta_2\cdot G\beta\gamma]/P_o$, is

$$\alpha = \frac{k_f t P_o}{(k_f t P_o = 1)} \quad (10)$$

For experiments in which $[\text{PLC-}\beta_2] \neq [G\beta\gamma]$, P_o was replaced by the average value of the two initial species:

$$P_o = \frac{[\text{PLC-}\beta_2]_o + [G\beta\gamma]_o}{2} \quad (11)$$

The justification for this approximation is described elsewhere (*30*). Analogous to steady-state equations, these apparent rates can also be translated into bulk phase values, as described above.

Dissociation rate constants (off rates) were measured under first-order conditions by first allowing the D−PLC-β_2·C−G$\beta\gamma$ complex to form, then chasing off D−PLC-β_2 with unlabeled PLC-β_2 or unlabeled Gα subunits. Data were fit to a simple exponential for the degree of association (α):

$$\alpha = e^{-k_r t} \quad \text{where} \quad \alpha \equiv \frac{[G\beta\gamma\cdot\text{PLC-}\beta]}{[G\beta\gamma]_o} \quad (12)$$

Since the dissociation rate is unimolecular, translation into bulk phase terms is not necessary.

Reconstitution of G$\beta\gamma$ Subunits into Bilayer Surfaces. In this work, we will be analyzing the lateral association between membrane-bound PLC-β_2 and G$\beta\gamma$ subunits. Typically, we reconstitute G$\beta\gamma$ as detailed below and add PLC-β_2 from a stock solution. We have previously characterized the membrane binding properties of this enzyme (*15*) and found that for the types of bilayers used in this study (PC:PS:PE 1:1:1 or PC:PS 2:1), all of the protein is completely bound by 100 μM lipid. Also, we have found binding to be independent of the presence of either PtdIns(4,5)P_2 or G$\beta\gamma$ subunits. Thus, the data we collected represents lateral association of membrane-bound species.

The goal of this experiment is to verify that; under the conditions that we will be doing the fluorescence studies,

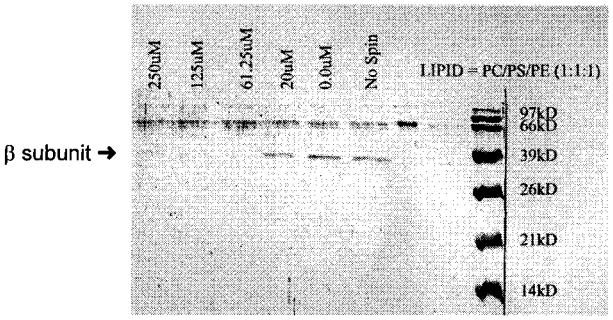

FIGURE 2: Reconstitution of G$\beta\gamma$ with sucrose-loaded vesicles (SLVs). G$\beta\gamma$ subunits were reconstituted by dilution into different concentrations of large unilamellar vesicles composed of 1:1:1 PC:PS:PE encapsulated with 160 mM sucrose (SLVs), allowed to incubate for 5 min, and sedimented for 30 min at 100000*g*. Samples of the supernatant were taken, subjected to SDS−PAGE, and visualized by Coomassie staining. The Gβ subunit of the G$\beta\gamma$ heterodimer appears in samples subjected to no spin or no lipid and disappears from the supernatant when the SLVs concentration exceeds 61.26 μM. The γ subunits run with the dye front and cannot be visualized.

all of the G$\beta\gamma$ subunits are membrane-bound. G$\beta\gamma$ subunits are assumed to partition readily into membranes, but since the protein is stored in detergent to prevent aggregation, it is possible that their affinity for membrane is reduced. The surfaces to be used [POPC:POPS:POPE 1:1:1 for fluorescence studies and with 2% PtdIns(4,5)P_2 for PLC-β_2 activity studies] were chosen as substrates because their surface charge and PE/PC concentrations are similar to those of the plasma membrane from rat liver (*27*). When they are reconstituted into bilayers, the amount of detergent is kept low enough so that the integrity of the bilayer remains intact (*31*) and is at least 100 times below the critical micelle concentration.

The efficiency of reconstitution is monitored by mixing G$\beta\gamma$ subunits LUVs loaded with 0.16 M sucrose at 0, 20, 61.25, 125, and 250 μM, incubating for 5 min, and centrifuging for 30 min at 100000*g* (*32*). Figure 2 shows that, at concentrations greater than 61.25 μM, more than 95% of the added G$\beta\gamma$ subunit is membrane-bound. Importantly, samples containing diluted G$\beta\gamma$ without vesicles showed an equivalent amount of protein in the supernatant as samples that were not subjected to centrifugation, indicating that G$\beta\gamma$ subunits do not aggregate and pellet under these conditions. Thus, G$\beta\gamma$ subunits were reconstituted into bilayers at lipid concentrations above 61 μM.

Activation of PLC-β_2 by G$\beta\gamma$ Subunits on Bilayer Surfaces. Activation of PLC-β_2 proteins by reconstituted G$\beta\gamma$ subunits was tested under conditions where the lipid concentration was constant. In Figure 3, we show the G$\beta\gamma$ activation profile of PLC-β_2 and, for comparison, the profile for PLC-β_1, which is not strongly activated by G$\beta\gamma$ subunits. The data in this figure show that PC:PS:PE with 2% PtdIns(4,5)-P_2 supports both PLC-β_2 enzymatic activity and its activation by G$\beta\gamma$ subunits and gives an activation profile comparable to those reported on other substrates (*14*, *33*−*41*).

RESULTS

Determination of PLC-β_2·G$\beta\gamma$ Affinity Using Fluorescence Resonance Energy Transfer. The affinity between G$\beta\gamma$ and an effector, in particular PLC-β_2, on bilayer surfaces has not been measured directly before, although estimates have been made by enzyme activity studies (*14*, *33*−*35*, *38*, *40*, *41*). Knowledge of this affinity is critical to understanding the possible physiological basis and selectivity of G$\beta\gamma$ signaling, as well as allowing us to evaluate the time-resolved kinetics of G$\beta\gamma$·PLC-β_2 association.

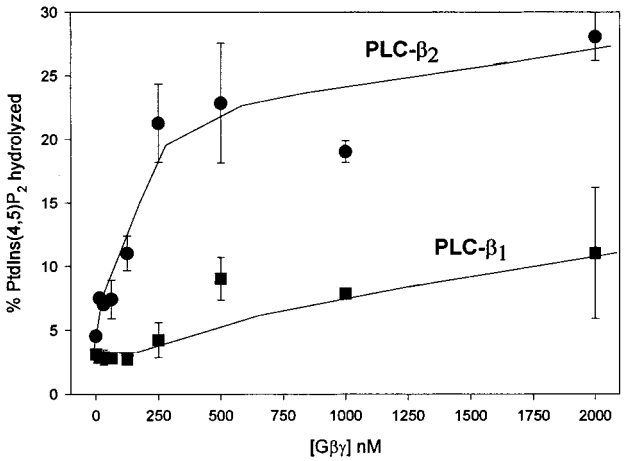

FIGURE 3: Activation of PLC-β_2 and PLC-β_1 by G$\beta\gamma$ subunits. Activation of PLC-β_2 and PLC-β_1 (for comparison) was performed as described using 1 mM PC:PS:PE 1:1:1 bilayers doped with 2% PtdIns(4,5)P_2. These results match previous studies showing preferential G$\beta\gamma$ activation of PLC-β_2 over PLC-β_1 on other substrate surfaces and demonstrate that activation is achieved in this model membrane system.

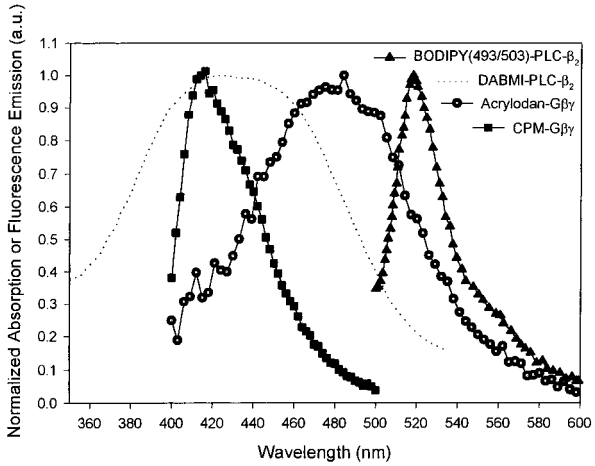

FIGURE 4: Overlap spectra of the energy transfer pairs used in this study.

We measured the affinity of the membrane-bound proteins (see refs *15* and Materials and Methods) by fluorescence resonance energy transfer (for background see ref *42*) by labeling PLC-β_2 and G$\beta\gamma$ with an energy donor−acceptor pair using either thiol-reactive or amine-reactive probes. Neither the PLC-β_2 activity or G$\beta\gamma$ activation profile is affected by labeling the two proteins with either type of reagent, and both types of probes give identical association data. For these studies, we have used the accepting group DABMI and used either acrylodan (A), coumarin (C), or BODIPY as fluorescence energy donors. The overlap spectra for these probes are shown in Figure 4 and R_0, the distance where 50% of the emission energy is lost to transfer, is similar for the three probes (35−41 Å; see ref *42*). Since DABMI and Dabcyl are not fluorescent, energy transfer is viewed as a decrease in the fluorescence of the donor. All three donor probes give approximately identical association

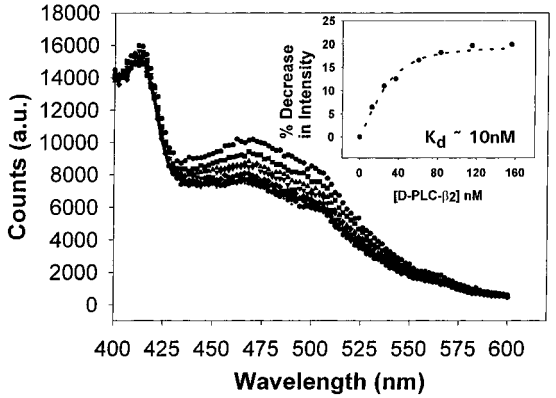

FIGURE 5: Association of DABMI-conjugated PLC-β_2 (D−PLC-β_2) with acrylodan-labeled G$\beta\gamma$ (A−$\beta\gamma$) as monitored by fluorescence resonance energy transfer. The decrease in the donor fluorescence of A−$\beta\gamma$ (acrylodan-G$\beta\gamma$), corrected for dilution as D−PLC-β_2 is sequentially titrated into a solution containing 75 nM A−$\beta\gamma$ reconstituted into 350 μM 1:1:1 PC:PS:PE large unilamellar vesicles (LUVs), where the concentrations of D−PLC-β_2 are 0 nM (●), 12 nM (■), 25 nM (▲), 37 nM (▼), 60 nM (◆), 83 nM (), 115 nM (⬢) and 156 nM (+). The 415 nm peak in the A−$\beta\gamma$ fluorescence emission spectrum is a scattering peak. The true peak of acrylodan fluorescence is at approximately 470 nm. Association between A−$\beta\gamma$ and D−PLC-β_2 is observed by plotting the percent decrease in fluorescence emission intensity versus concentration of D−PLC-β_2 added (shown in inset). Control studies using buffer, unlabeled PLC-β_2, or D-PLC-β_1 (which is not significantly activated by G$\beta\gamma$ subunits; (*11*, *35*, *38*), failed to decrease the emission of A−$\beta\gamma$. Data are transformed in terms of degree of association (α) and fit to a bimolecular association curve (see Materials and Methods), giving an apparent dissociation constant of approximately 10 nM.

data. We present data for all three types of probes, but we note that out of the three types of probe donors, acrylodan-labeled proteins were environmentally sensitive and had a lower signal compared to the other two.

Figure 5 shows the decrease in acrylodan−G$\beta\gamma$ (75 nM on 350 μM lipid) emission, corrected for dilution, as D−PLC-β_2 is sequentially added. The decrease in acrylodan fluorescence is interpreted to be due to fluorescence resonance energy transfer to the DABMI moiety on PLC-β_2 as it associates with A−$\beta\gamma$ (see below). The extent of this decrease is in a range expected for two proteins of this size with this particular energy transfer pair. Also, this extent was easily reproducible over several protein preparations. We present data for this probe to show the contribution of lipid background and the quality of the data collected. We note that the coumarin and BODIPY probes had a much stronger emission signal and less background contribution.

Fluorescence resonance energy transfer was confirmed by several sets of control studies. First, substituting D−PLC-β_2 dialysis buffer, unmodified PLC-β_2, or PLC-β_1 (which is not significantly activated by G$\beta\gamma$ subunits; *11*, *35*, *38*) for D-PLC-β_2 did not change the emission intensity of A−$\beta\gamma$ when corrected for dilution. Second, the decrease in fluorescence intensity could be blocked by preincubating G$\beta\gamma$ with excess unlabeled PLC-β_2 (see below). Third, fluorescence energy transfer was confirmed by time-resolved methods (data not shown). We found that the decrease in the fluorescence lifetime of A−$\beta\gamma$ is comparable to the decrease in the fluorescence intensity (10−15%) when saturating amounts of D−PLC-β_2 are present. The decay curves were multiexponential, reflecting either a distribution of labeling sites (see Materials and Methods), rotamer populations, or protein dimers. We did not analyze the heterogeneity of the system or extract the dissociation constant from these data.

The apparent K_d for the association between D−PLC-β_2 and A−$\beta\gamma$ was determined by plotting the percent decrease in spectral area versus concentration of D−PLC-β_2 and fitting to a simple bimolecular association curve for two proteins. A value of $K_d = 10$ nM was obtained. A similar value was obtained by substituting acrylodan-labeled His_6-G$\beta_1\gamma_2$ for the bovine brain preparation of G$\beta\gamma$, which is a mixture of Gβ and Gγ isotypes (data not shown). This result indicates a lack of specificity of a particular G$\beta\gamma$ pair for PLC-β_2.

Since the apparent K_d value will vary with the amount of lipid used in the experiment, it is more helpful and understandable to translate this apparent two-dimensional K_d to the value one would obtain for the two proteins interacting in bulk solution. This analysis gives $K_d = 3.2$ μM (see Materials and Methods).

Monitoring the association between G$\beta\gamma$ and PLC-β_2 could also be achieved by using different donor and acceptor probes, and similar values for the K_d were obtained as mentioned above. Thus, the systematic changes in resonance energy transfer using several probe pairs in the protein titrations, the reproducibility of the K_d values obtained, and the consistency of the control studies convinced us that fluorescence is accurately reporting PLC-β_2·G$\beta\gamma$ interactions. We note that we also obtained a similar dissociation constant using a non-FRET method in which we labeled G$\beta\gamma$ subunits with the environmentally sensitive probes dansyl chloride or acrylodan and monitored the change in their emission when unlabeled PLC-β_2 was added. This method was successful when the probe attached on a G$\beta\gamma$ site that was close or altered by PLC-β_2 interaction, which was not always the case. Nevertheless, the observation that a second fluorescent-based method yields a similar K_d further shows that we are viewing protein−protein association on the membrane surface.

Estimation of Membrane Surface Crowding. It is important to note that the titration shown in Figure 5 was done at PLC-β_2 and G$\beta\gamma$ concentrations that are far below concentrations where nonspecific interactions due to surface crowding would occur. These concentrations can be estimated from the available lipid surface area and the molecular areas of the two proteins. For PLC-β_2 and G$\beta\gamma$, these latter parameters are estimated from the crystal structures of the catalytic region of PLC-δ_1 [150 × 50 × 50 Å (lwh)] (*43*), and the structure of G$\beta\gamma$ (50 × 50 × 50 Å) (*44*, *45*). For example, the available surface area of lipid for 350 μM PC:PS:PE in a 100 μL sample is 7.87×10^{17} Å^2, assuming the molecular area of the lipid headgroups is 75 A^2/molecule (see ref *27*) and keeping in mind that only the upper leaflet of the membrane is available for protein binding. Since the membrane partition coefficients of PLC and G$\beta\gamma$ are less than 100 μM, then at 350 μM lipid, all species would be bound. If we use equimolar concentrations of PLC and G$\beta\gamma$, then 1.35×10^{14} molecules of PLC and G$\beta\gamma$ (or ~1.2 μM each) will completely cover the surface. This value sets an upper limit on the concentrations that should be used in these titrations.

Dependence of PLC-β_2·G$\beta\gamma$ Apparent Affinities on Membrane Surface Area. To verify that we are viewing protein−

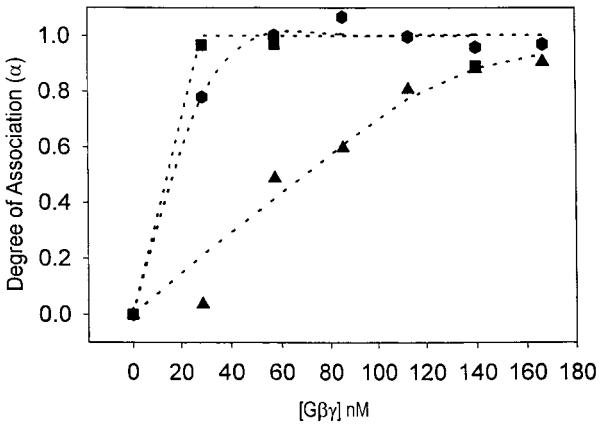

FIGURE 6: Effect of membrane surface area on PLC-β_2 and G$\beta\gamma$ association: dependence of the degree of association (α) between BODIPY 493/503 methyl bromide-conjugated PLC-β_2 (BODIPY−PLC-β_2) and DABMI-conjugated G$\beta\gamma$ (D−$\beta\gamma$) on the amount of available surface. In this experiment D−$\beta\gamma$ is titrated into ~25 nM BODIPY−PLC-β_2 reconstituted with either 300 μM (■), 625 μM (●), or 1000 μM (▲) 1:1:1 PC/PS/PE large unilamellar vesicles (LUVs). Increasing the lipid concentration increases the effective surface area on which PLC-β_2 and G$\beta\gamma$ can interact.

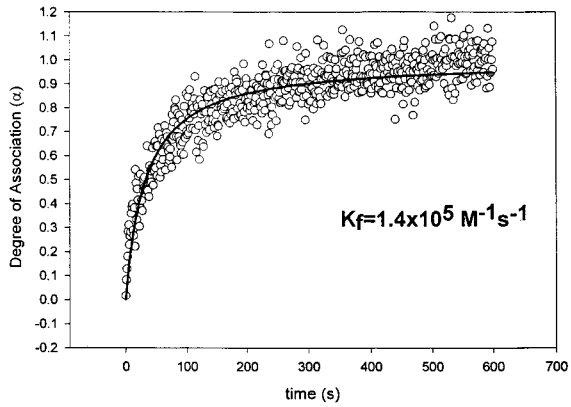

FIGURE 7: Rate of association of PLC-β_2 with G$\beta\gamma$. The rate at which DABMI-conjugated PLC-β_2 (D−PLC-β_2) associates with coumarin-conjugated G$\beta\gamma$ (C−$\beta\gamma$) was investigated by reconstituting 25 nM C−$\beta\gamma$ into 500 μM 1:1:1 PC/PS/PE large unilamellar vesicles (LUVs) and by monitoring the change in fluorescence with time after D−PLC-β_2 was mixed with reconstituted C−$\beta\gamma$, using a stopped-flow fluorometer. The forward rate of association (k_f) was monitored under second-order conditions, in which the initial concentrations of both proteins are similar. Data were analyzed by transforming the fluorescence decrease accompanying D−PLC-β_2 association with C−$\beta\gamma$ (a result of a increase of fluorescence resonance energy transfer activity) in terms of the degree of association (see Materials and Methods). This figure shows the time dependence of the degree of association (α) of 400 nM D−PLC-β_2 with 25 nM C−$\beta\gamma$ reconstituted into 500 μM LUVs. k_f was obtained by fitting the data as described under Materials and Methods.

protein association on membrane surfaces, we varied the effective concentration of the two proteins by varying the lipid concentration. In Figure 6 we show a study where DABMI-labeled G$\beta\gamma$ (DABMI−G$\beta\gamma$) was titrated into BODIPY 493/503 methyl bromide-labeled PLC-β_2 (BODIPY−PLC-β_2). As the concentration of LUVs is increased, more DABMI−G$\beta\gamma$ was needed to reach saturation. Thus, the amount of membrane surface area available directly affects the degree of association of the two proteins, which is consistent with the premise of two proteins interacting laterally on the membrane surface. Moreover, it illustrates the possible importance membrane compartmentalization could play in intracellular signaling by decreasing the effective sampling volume.

Kinetics of the Association and Dissociation of PLC-β_2 with G$\beta\gamma$. Determination of the on rate of the PLC-β_2·G$\beta\gamma$ complex was done by adding PLC-β_2 into a solution containing G$\beta\gamma$ reconstituted on membranes. The association rate consists of the diffusion rate of PLC-β_2 in aqueous solution, the membrane binding rate of PLC-β_2, the lateral diffusion rate of both PLC-β_2 and G$\beta\gamma$ on the membrane surface, and the complexation rate. The first and third rates can be estimated from literature (e.g. ref *46*) and the rate of PLC-β_2 association to membrane surface was estimated from stopped-flow fluorescence measurements (data not shown). The diffusion rate of PLC-β_2 in aqueous solution and the rate of membrane binding of PLC-β_2 are several orders of magnitude faster than the on rate measured below. Thus, the PLC-β_2·G$\beta\gamma$ association rate can be described by the rates of membrane diffusion and complexation.

The measurement of the on rate of the complex was done by monitoring the change in fluorescence with time after DABMI-labeled PLC-β_2 (D−PLC-β_2) was mixed with coumarin-labeled G$\beta\gamma$ (C−$\beta\gamma$) reconstituted into LUVs, using a stopped-flow fluorometer. C−$\beta\gamma$ was excited at 350 nm and the emission was observed at 460 nm. The 10−15% fluorescence decrease that accompanies the association of D−PLC-β_2 with C−$\beta\gamma$ due to energy transfer was monitored under second-order conditions, where the initial concentrations of both proteins are similar. Figure 7 shows the association rate kinetics of complex formation in buffer with 25 nM C−$\beta\gamma$ reconstituted into 500 μM PC:PS:PE and 400 nM D−PLC-β_2. The k_f value, which was calculated from eq 4 (see Materials and Methods), is 1.4×10^5 M^{-1} s^{-1} for this experiment. As expected, similar rate constants of association were obtained for varying concentrations of C−$\beta\gamma$ and D−PLC-β_2 (see Table 1) to give a mean value of $(2.0 \pm 0.9) \times 10^5$ M^{-1} s^{-1} with a standard error of the mean calculated from 4−6 repetitions of each experiment for all of the data collected ($n = 7$). This apparent two-dimensional association rate constant, if put into bulk phase terms, will decrease by ~100 and will fall below the range of diffusion-limited associations, indicative of conformation changes that may occur during complexation (*47*, *48*). However, this rate still corresponds to very short times for activation (less than microseconds) under the conditions of our activity assays.

Table 1: Values of k_f at Varying Protein Concentrations

[$\beta\gamma$] (nM)	[PLC-β_2] (nM)	[PC:PS:PE] (μM)	$k_f \times 10^5$ (M·s)$^{-1}$
25	400	500	1.6
25	300	500	1.2
25	200	500	2.9
35	76	500	2.5

Measurement of the off rate of the complex was done under first-order conditions by first allowing the D−PLC-β_2·C−$\beta\gamma$ complex to form on PC:PS:PE LUVs, and then chasing off the D−PLC-β_2 with 10−20 times the concentration of unlabeled PLC-β_2. The disruption of the D−PLC-β_2·C−$\beta\gamma$ complex by PLC-β_2 can be monitored by observing the increase in fluorescence with time after mixing as transfer from the coumarin probe on G$\beta\gamma$ to the DABMI probe on

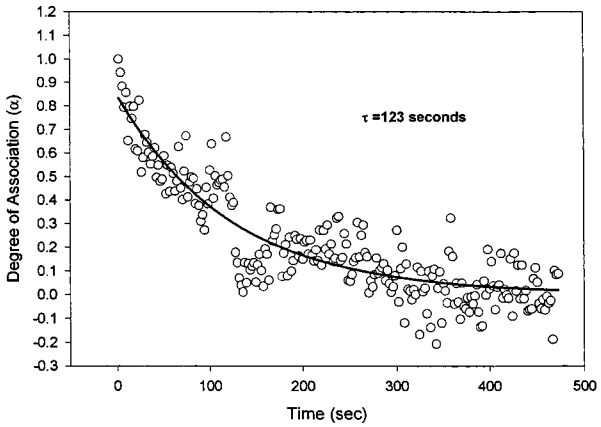

FIGURE 8: Rate of dissociation of PLC-β_2 from G$\beta\gamma$. The rate at which DABMI-conjugated PLC-β_2 (D−PLC-β_2) dissociates from coumarin-conjugated G$\beta\gamma$ (C−$\beta\gamma$) was investigated by first incubating 100 nM D−PLC-β_2 with 25 nM C−$\beta\gamma$ reconstituted into 500 μM 1:1:1 PC/PS/PE large unilamellar vesicles (LUVs) and then chasing off D−PLC-β_2 from the D−PLC-β_2·C−$\beta\gamma$ complex with the addition at $t = 0$ of 2 μM unconjugated PLC-β; the change in fluorescence with time after mixing was monitored with a K2 spectrofluorometer. Data were analyzed by transforming the fluorescence increase accompanying D−PLC-β_2 dissociation from C−$\beta\gamma$ (a result of a decrease in fluorescence resonance energy transfer activity) in terms of the degree of association (α) (see Materials and Methods). This figure shows the time course of dissociation of D−PLC-β_2 from C−$\beta\gamma$ following the addition of excess unlabeled PLC-β_2.

PLC-β_2 is concomitantly reduced. Substituting buffer or unlabeled PLC-β_2 did not alter the C−$\beta\gamma$ intensity, indicating that the increase in fluorescence is specifically due to a disruption of resonance energy transfer from coumarin-labeled G$\beta\gamma$ to DABMI-labeled PLC-β_2. Figure 8 shows the dissociation rate kinetics of D−PLC-β_2·C−$\beta\gamma$ (at 111 and 37 nM, respectively) in 500 μM LUVs and 2 μM unlabeled PLC-β_2. Identical results were obtained with 1 μM unlabeled PLC-β_2. Because the maximum signal change was low, ~10%, significant data could only be obtained by using high concentrations of unlabeled PLC-β_2 to dissociate the complex. The k_r value, calculated from eq 6 (see Materials and Methods), was found to be 8.13×10^{-3} s^{-1} for this experiment, or a lifetime of $\tau = 1/k_r = 123$ s. Similar rate constants of dissociation were measured for several experiments, with a mean value of $(7.9 \pm 0.3) \times 10^{-3}$ s^{-1}. The standard error of the mean (σ) was calculated from repetitions of each experiment for all of the data collected ($n = 5$). Thus, the average lifetime (τ) for the G$\beta\gamma$·PLC-β_2 interaction is $\tau \equiv 1/k_r = 1/(7.9 \times 10^{-3}\ s^{-1}) \approx 126.5$ s. Since the dissociation rate is independent of concentration, no corrections for the reduction of dimensionality are required.

Given an on rate constant of $k_f = (2.0 \pm 0.9) \times 10^5$ M^{-1} s^{-1} and an off rate constant of $k_r = (7.9 \pm 0.3) \times 10^{-3}$ s^{-1}, the apparent equilibrium dissociation constant is calculated as $K_d = k_r/k_f = 40 \pm 32$ nM. The calculated $K_d = 40$ nM from the kinetics measurements falls into the range of values calculated from direct measurements (~10 nM). By use of the bulk phase value of K_d, the free energy of interaction can be calculated by converting the concentrations of species into mole fractions including solvent (water at 55 M) giving $\Delta G_{int} = -4.2$ kcal/mol.

Gα_{i1}(GDP) Can Functionally Deactivate G$\beta\gamma$·PLC-β_2 without Physically Disrupting the Complex. We attempted to measure the off rate of G$\beta\gamma$·PLC-β_2 complexes by adding a 20-fold excess of unlabeled recombinant Gα_{i1}(GDP). This high concentration (2 μM) of Gα_{i1}(GDP) would be expected to completely bind all the G$\beta\gamma$ and displace PLC-β_2. Unexpectedly, the addition of Gα_{i1}(GDP) did not disrupt the PLC-β_2·G$\beta\gamma$ complex (data not shown).

We also tested whether Gα_{i1}(GDP) could block D−PLC-β_2·C−$\beta\gamma$ association. To accomplish this, we measured the association of D−PLC-β_2 to membrane-bound C−$\beta\gamma$ that had been preincubated either with buffer or with a 20-fold molar excess of Gα_{i1}. The results of this study are presented in Figure 9A. These data show that the presence of Gα_{i1}-(GDP) failed to block the $\beta\gamma$−PLC-β_2 association. To verify that the fluorescence experiment is reflecting D−PLC-β_2·C−$\beta\gamma$ association as seen by FRET, we show that dilution with unlabeled PLC-β_2 reduces this effect.

To rule out the trivial explanation that the proteins were inactive or that the fluorescent labels interfered with the experiment, we tested to see whether Gα_{i1}(GDP) could prevent activation of D−PLC-β_2 by C−$\beta\gamma$. The results, presented in Figure 9B, show that indeed preincubation of an identical amount of Gα_{i1}(GDP) with C−$\beta\gamma$ prevents activation of D−PLC-β_2. These results suggest that Gα_{i1}-(GDP) can functionally turn off G$\beta\gamma$ enzymatic activation of PLC-β_2 without physically displacing PLC-β_2 from G$\beta\gamma$.

Gα_o(GDP) Can Form Complexes with $\beta\gamma$·PLC-β_2. To investigate the mechanism by which Gα_{i1} functionally deactivates PLC-β_2 without displacing G$\beta\gamma$, we tested whether G$\beta\gamma$ can bind Gα and PLC-β_2 simultaneously. We measured the association of D−PLC-β_2 with coumarin-labeled Gα_o(GDP)$\beta\gamma$ heterotrimer purified from bovine brain (C−G$\alpha_o\beta\gamma$) on membrane bilayers. Figure 10 presents the percent decrease in C−G$\alpha_o\beta\gamma$ fluorescence due to energy transfer to D−PLC-β_2. These data show that this association does occur, although the measured affinity ($K_d = 1100$ nM) is some 27−110-fold weaker than the affinity of PLC-β_2 for G$\beta\gamma$ subunits alone ($K_d = 10-40$ nM) at the same lipid concentration. In addition, activity measurements performed in parallel show that, as expected, the G protein heterotrimer does not activate PLC-β_2 (data not shown).

Deactivation of PLC-β_2·G$\beta\gamma$ by Gα_{i1}(GDP) Can Occur at a Faster Rate than the Physical Dissociation of G$\beta\gamma$ from PLC-β_2. We tested whether Gα can deactivate G$\beta\gamma$·PLC-β_2 at a rate much faster than the rate expected from a simple displacement mechanism, in which Gα_{i1} must wait for G$\beta\gamma$ to dissociate from PLC-β_2 before it can bind G$\beta\gamma$. From our fluorescence studies, the rate of dissociation of PLC-β_2 from G$\beta\gamma$ gives an effective lifetime (τ) equal to $\tau = 1/k_r = 126$ s. Thus, we would expect a similar rate of deactivation of G$\beta\gamma$-stimulated PLC-β_2 activity by Gα_{i1} if deactivation operates through a simple displacement mechanism. Using an activity assay under conditions comparable to those used in our fluorescence measurements, we measured the change in the extent of PLC-β_2 activation by G$\beta\gamma$ following the addition of excess Gα_{i1}. Points were taken at times much shorter (30 s) than the dissociation lifetime of PLC-β_2·G$\beta\gamma$ complex and slower than the reported association rate of Gα-(GDP) and G$\beta\gamma$ of $k_f = 4.1$ s^{-1} (*49*). The results are presented in Figure 11. The data clearly show Gα_{i1}(GDP) can rapidly deactivate G$\beta\gamma$-stimulated PLC-β_2 activity, within seconds rather than minutes, and at a rate faster than the physical dissociation as measured by fluorescence.

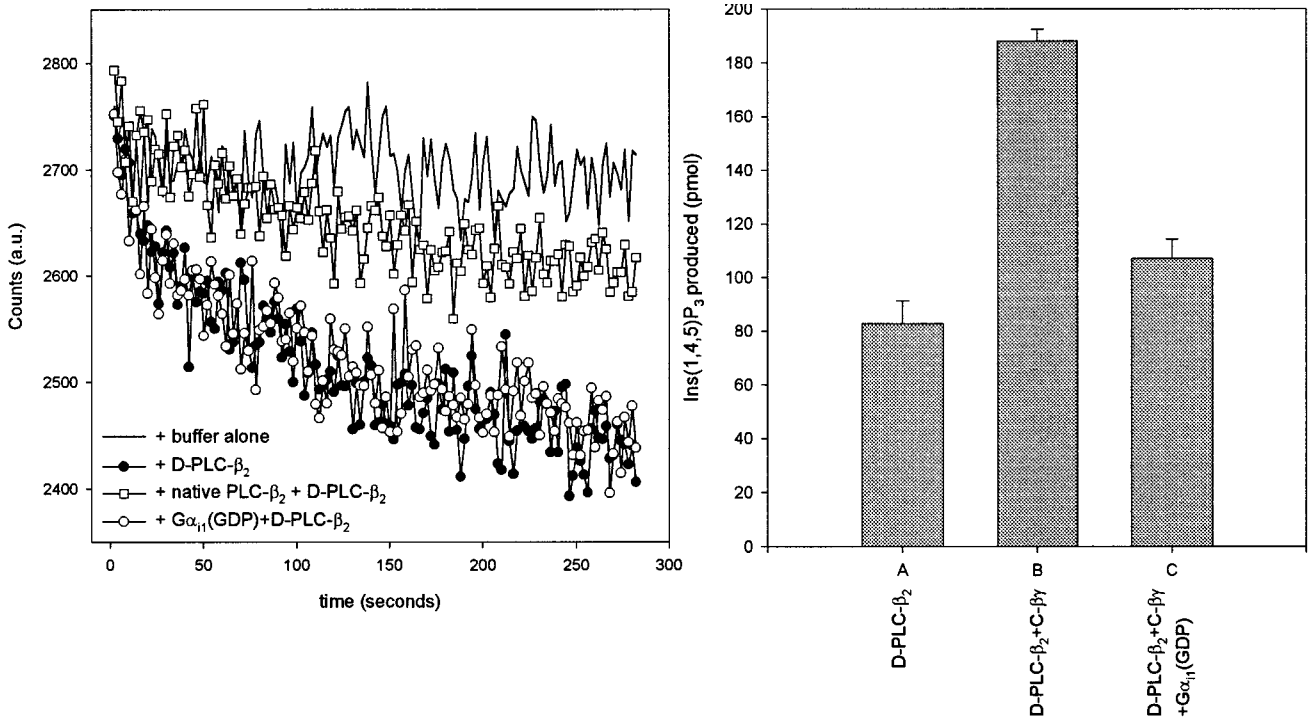

FIGURE 9: (A) Gα_{i1} does not displace PLC-β_2 from G$\beta\gamma$. We investigated whether Gα_{i1} or unlabeled PLC-β_2 could block the association of DABMI-conjugated PLC-β_2 (D−PLC-β_2) with courmarin-labeled G$\beta\gamma$ (C−$\beta\gamma$). C−$\beta\gamma$ (100 nM) was reconstituted into 250 μM 1:1:1 PC:PS:PE large unilamellar vesicles (LUVs), and the change in fluorescence emission with time was monitored after mixing with buffer (—), with 700 nM D−PLC-β_2 (●) alone, with D−PLC-β_2 plus C−$\beta\gamma$ preincubated with 2 μM rGα_{i1} (○) or with D−PLC-β_2 plus 1.5 μM unlabeled PLC-β_2 (□). (B) Preincubating 2 μM Gα_{i1} with 800 nM C−$\beta\gamma$ could block activation of 100 nM D−PLC-β_2 by C−$\beta\gamma$ under conditions similar to those of the fluorescence experiment. PLC activity was determined by reconstituting the enzyme with 1 mM extruded phospholipid vesicles composed of a mixture of 1:1:1 PC/PS/PE with 2 mol % PtdIns(4,5)P_2 as described (*15*). Vesicles were doped with approximately 8000 cpm/sample [^{3}H]PtdIns(4,5)P_2 (New England Nuclear) to follow the PLC-catalyzed hydrolysis of PtdIns(4,5)P_2.

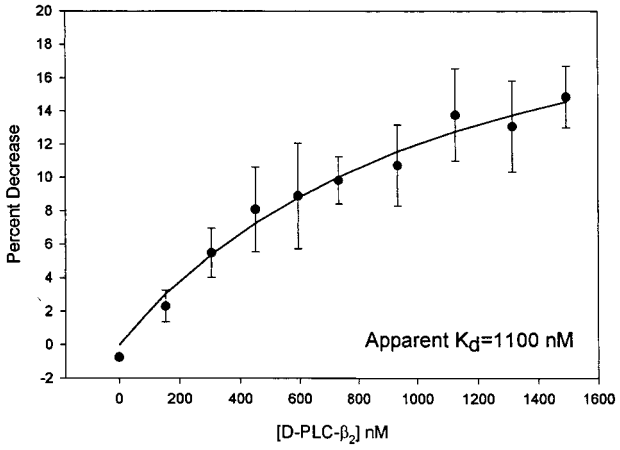

FIGURE 10: PLC-β_2 can bind to the G protein heterotrimer G$\alpha_o\beta\gamma$. We investigated whether PLC-β_2 can association with GDP-bound G protein heterotrimer [Gα_o(GDP)$\beta\gamma$] purified from cholate extracts of bovine brain (see Materials and Methods). G$\alpha_o\beta\gamma$ conjugated to CPM (C−G$\alpha_o\beta\gamma$) was reconstituted into 250 μM 1:1:1 PC:PS:PE LUVs, and DABMI-conjugated PLC-β_2 was sequentially added. Association between C−G$\alpha_o\beta\gamma$ and D−PLC-β_2 is observed by plotting the percent decrease in fluorescence emission intensity versus concentration of D−PLC-β_2 added. Shown is the fit to an apparent two-dimensional K_d (1150 nM), which translates to a bulk phase $K_d \sim 200$ μM (see Materials and Methods).

For comparison, the theoretical expected decrease in G$\beta\gamma$-stimulated PLC-β_2 activity, assuming a deactivation lifetime equal to the dissociation lifetime of G$\beta\gamma$ from PLC-β_2 ($\tau = 1/k_r = 126$ s), is also shown in Figure 11. In this approximation, we assumed that the concentration of G$\beta\gamma$·PLC-β_2 in the assay following the addition of Gα_{i1} decreases exponentially with a lifetime $\tau = 126$ s. Neglecting the basal activity of the unassociated PLC-β_2 and approximating the activity of the associated G$\beta\gamma$·PLC-β_2 complex as A (activity/time), we estimate the expected amount of total activity that occurs within the 30 s of our assay if Gα_{i1} reverses G$\beta\gamma$-stimulated PLC-β_2 activity by simply displacing the PLC-β_2 from the G$\beta\gamma$ subunit:

$$\% \text{ full activation} = \frac{\int_0^t A e^{-t/\tau}\, dt}{\int_0^t A\, dt}(100) \Rightarrow \frac{\tau}{t}(1 - e^{-t/\tau})(100) \quad (13)$$

We find that if Gα(GDP) deactivates by displacing PLC-β_2 from G$\beta\gamma$, then we should only see ~10% reversal of full activation and not the ~73% reversal that is experimentally obtained. We conclude that deactivation by Gα(GDP) subunits does not occur through a displacement mechanism.

DISCUSSION

In an effort to better understand the mechanism of G$\beta\gamma$-mediated effector signaling, we used fluorescence spectroscopy to characterize the interaction of G$\beta\gamma$ subunits with PLC-β_2 on membrane surfaces, the kinetic rates governing the interaction, and the role of the Gα subunit of heterotrimeric G proteins in controlling the lifetime G$\beta\gamma$·phospholipase Cβ_2 complex. We have conducted these studies at a high enough lipid concentration so that all of the proteins are membrane-bound and we can view their lateral association.

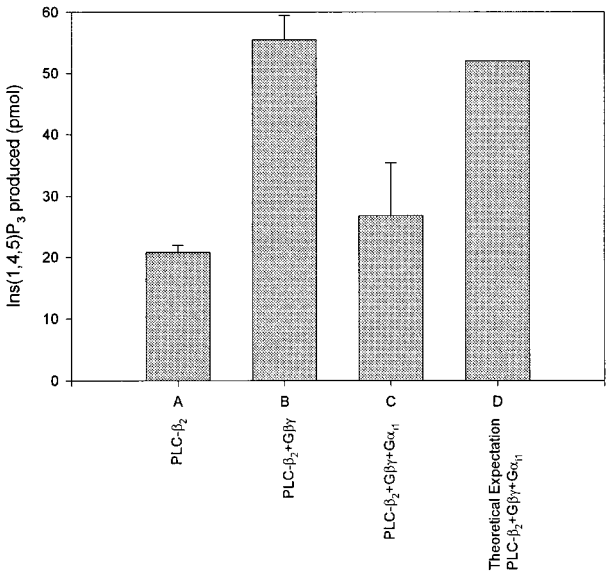

FIGURE 11: $G\alpha_{i1}$(GDP) deactives $G\beta\gamma$-stimulated PLC-β_2 activity faster than expected by simple PLC-β_2·$G\beta\gamma$ dissociation. Samples containing only vesicle substrate, $G\beta\gamma$, and PLC-β_2 were incubated at 37 °C for 5 min to allow the sample temperature to equilibrate and $G\beta\gamma$ sufficient time to complex with PLC-β_2. The sample contained 133 μM 1:4 PtdIns(4,5)P_2:PE sonicated vesicle substrate, 400 nM $G\beta\gamma$ or $G\beta\gamma$ buffer, and 100 nM PLC-β_2. Vesicles were doped with approximately 8000 cpm/sample [^{3}H]PtdIns(4,5)P_2 to follow the PLC-catalyzed hydrolysis of PtdIns(4,5)P_2. Reactions were initiated by mixing with a calcium solution (37 °C) containing either boiled or nonboiled $G\alpha_{i1}$ (2 μM final). Reactions were terminated after 30 s by adding ice-cold 10% TCA and then 2% BSA, incubated on ice for 5 min, and centrifuged, and the liberated [^{3}H]Ins(1,4,5)P_3 was counted. Theoretical expected activity was calculated as detailed in the text.

Previous studies have shown that membrane binding of PLC-β_2 is independent of the presence of PtdIns(4,5)P_2 or $G\beta\gamma$ subunits in the vesicles and PLC-β_2 is not activated by recruitment to the membrane by substrate or $G\beta\gamma$ subunits (*15*, *21*, *50*).

We first measured the affinity of $G\beta\gamma$ for PLC-β_2 on a model membrane surface and found that the apparent K_d is approximately 10 nM, which correlates well with the activation profile observed by us and others (*33*, *35*). This value corresponds to a bulk phase K_d of 3.2 μM when the concentration of the proteins on the membrane surface are considered (see Materials and Methods). While this is the first reported direct measurement of the association between a G protein subunit and an effector on a membrane surface, there is a recent report of the association between $G\beta\gamma$ and a portion of the carboxyl terminus of GST-Kir3.4 inward rectifier K^+ channel subunits immobilized by anti-GST to a biosensor chip (*51*). These measurements give a K_d of ~800 nM, and 1−2 μM for the full-length GST-Kir3.1 carboxyl-terminal fusion protein, which are in line with the EC_{50} of ~1 μM obtained for activation by transducin $\beta\gamma$ in a detergent-free system. Thus, these two $G\beta\gamma$ effectors have similar affinities.

We corroborated our steady-state measurement of the K_d for $G\beta\gamma$·PLC-β_2 (10 nM) with the value independently calculated from the on and off rate constants (40 ± 32 nM), and found it to be in good agreement. The measured on rate constant of PLC-β_2 to $G\beta\gamma$ is slower than the diffusion-limited range for association of membrane proteins, indicating that slower, conformational changes occur when the two proteins dock. However, this on rate constant is generally consistent with the fast activation of PLC-β_2 in vitro and with the observed fast onset of Ca^{2+} ion release and Ins(1,4,5)P_3 generation following receptor-stimulated release of pertussis and cholera toxin-sensitive PI-PLC activity (*52*).

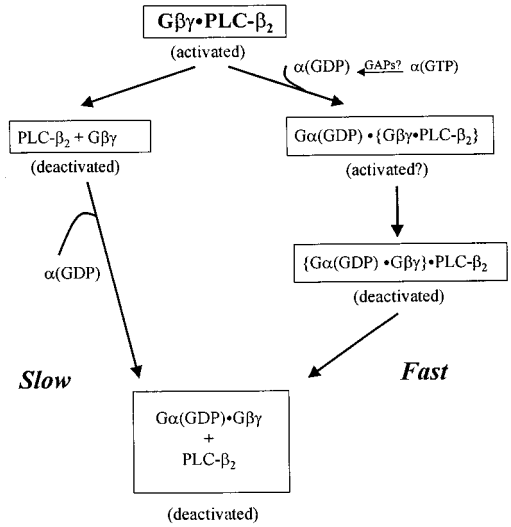

FIGURE 12: Model of deactivation pathways for $G\beta\gamma$-mediated PLC-β_2 signaling. Our studies indicate two mechanisms for PLC-β_2 deactivation. In the slow process (i.e., t = 126 s), the PLC-β_2·$G\beta\gamma$ complex physically dissociates, allowing α(GDP) to rebind to $G\beta\gamma$. In the fast process (i.e., t < 30 s), α(GDP) subunits bind directly to the PLC-β_2·$G\beta\gamma$ complex and rapidly deactivate PLC-β_2. In this case, the initial high interaction energy is between PLC-β_2 and $G\beta\gamma$, as denoted by braces. Physical association of α(GDP) to the complex allows direct switching of this energy to the α-(GDP)·$\beta\gamma$ association region.

Measurement of the off rate constant for the $G\beta\gamma$·PLC-β_2 complex gave a lifetime ($\tau = 1/k_r$) of 126 s. This long time is in the same range as that measured for the dissociation of $G\beta\gamma$ and the carboxyl terminus of the GST-Kir3.4 inward rectifier K^+ channel (*51*). Our value is qualitatively similar to k_r calculated from the steady-state determination of the dissociation constant (K_d) and the forward rate constant (i.e., 2×10^{-3} s^{-1}). These data demonstrate that the intrinsic lifetime of $G\beta\gamma$·effector complexes is long-lived and on the order of minutes. Thus, in the cell, $G\beta\gamma$-stimulated PLC-β_2 activity would be sustained for minutes, without some deactivating factor(s).

A likely candidate for PLC-β_2·$G\beta\gamma$ deactivators are inactive α(GDP) subunits. Here, we present a model in which α subunits directly deactivate $G\beta\gamma$-stimulated PLC-β_2 activity by binding to the activated $G\beta\gamma$·PLC-β_2 complex, which causes deactivation without effector displacement (Figure 12). This model is supported by the observation that $G\alpha_{i1}$ cannot block $G\beta\gamma$ association with PLC-β_2 complex but prevents $G\beta\gamma$ activation of PLC-β_2. Also, the rate of deactivation of $G\beta\gamma$-stimulated PLC-β_2 activity by $G\alpha_{i1}$-(GDP) is much faster than the rate expected from a simple effector-displacement mechanism.

The proposed mechanism depicted in Figure 12 can be rationalized in terms of the possible interaction sites between the proteins. Comparison of the crystal structure of the $G\alpha_{i1}$-(GDP)$\beta_1\gamma_2$ heterotrimer (*44*) with a region within the G protein β1 subunit (T327−N340) identified by Zhang and co-workers (*53*) as contributing to $G\beta\gamma$-stimulated PLC-β_2

activity shows that the putative PLC-β_2 binding site on Gβγ is not completely blocked by the interface between Gα and Gβγ in the heterotrimer structure. Strengthening this argument is evidence that Gβγ does not undergo allosteric changes when it dissociates from Gα (*45*). Thus, it is reasonable to propose that the Gα binding site on Gβγ may not be occluded in the activated Gβγ·PLC-β_2 complex. Our observation that PLC-β_2 can bind the isolated $G\alpha_o\beta\gamma$ heterotrimer supports this idea.

In our model, binding of Gα(GDP) to the activated Gβγ·PLC-β_2 complex, presumably to the Gβ subunit, results in rapid deactivation by switching the free energy from the Gβγ·PLC-β_2 interaction in favor of Gα(GDP)·Gβγ interaction. The energy involved in this switching, estimated from the K_d values, is 1.9 kcal/mol. This mechanism provides a novel mechanism by which Gα could rapidly shut down Gβγ-stimulated PLC-β_2 signaling. The rate of Gβγ-stimulated PLC-β_2 deactivation could occur rapidly and be under the direct control of Gα. The rate of deactivation would then depend on the association rate of Gα with the activated Gβγ·PLC-β_2 complex, and hence the local concentration of the Gα(GDP). The local concentration of Gα(GDP) depends on the intrinsic GTPase activity of the specific α subunit, which could also be regulated by GTPase activating proteins (GAPs), such as the newly discovered regulators of G protein signaling (RGS) proteins.

The kinetics of PLC-β_2 signaling in cells has not been extensively studied. Indeed, there may be some circumstances where sustained PLC-β_2 activity is required, e.g., a relatively long cellular response. However, our results here show that cells could also easily control the rate of deactivation of Gβγ-stimulated PLC-β_2 activity by temporally controlling the local concentration of deactivated α subunits that can bind to the activated PLC-β_2·Gβγ complex. Support for regulation of βγ·effector signaling comes from studies showing that both yeast Sst2 and mammalian RGS can regulate pheromone signaling, which is transmitted through Gβγ (*54*). The concentration of Gα(GDP) depends on the α subtype, since each has a distinct rate of GTP hydrolysis, and on the local type and concentrations of either RGS proteins or other GAPs.

In order for the deactivation model proposed in Figure 12 to be operative in cells, α(GDP) subunits must be at appropriate concentrations to bind to the PLC-β_2·Gβγ complex. However, the binding constant of Gα subunits for the PLC-β_2·Gβγ complex is not clear. Although our measured affinity of PLC-β_2 for α(GDP)·βγ implies a relatively low affinity, this affinity comprises of the binding energy of PLC-β_2 to the heterotrimer, the equilibrium constant for the switching of the high-energy interaction from α(GDP)·βγ to PLC-β_2·Gβγ, and the dissociation constant of α(GDP) from PLC-β_2·Gβγ. In parallel, the association of α(GDP) to PLC-β_2·Gβγ comprises the initial binding of α(GDP) to the complex, the switching of the high-energy interactions from PLC-β_2·Gβγ to α(GDP)·βγ, and dissociation of PLC-β_2. Our steady-state measurements are unable to isolate these coupled equilibria, and it is entirely reasonable that the deactivation mechanism in Figure 12 can occur with some frequency. In cells, there is a critical balance between these components [α(GDP), βγ, and PLC-β_2] and overexpression of one of these species, or a component that regulates their concentration, such as RGS protein, could alter the kinetics of PLC-β_2 signaling.

It is also worth considering that while α subunits show some degree of effector specificity, different Gβγ subunits isotypes show only marginal specificity. Thus, PLC-β_2 could be activated in response to a variety of signals and deactivated by different Gα subunits, providing a basis for cross-talk from different α subtypes and receptors. The relatively weak affinities (approximately micromolar) between Gβγ subunits and the PLC-β_2 effector as well as the carboxyl terminus of the Kir3.4 inward rectifier K^+ channel (*55*) indicate that a high local concentration of βγ subunits is required for signal stimulation, and if a comparable amount of α(GDP) is rapidly generated, then activation of these effectors could be readily extinguished. Future in vivo studies must be done to determine whether these events occur in cells.

ACKNOWLEDGMENT

We express our gratitude to Dr. Alfred G. Gilman and Dr. Roger K. Sunahara (University of Texas Southwestern Medical Center at Dallas) for their generous gift of the JM109 cell strain cotransformed with pQE-6-$G_i\alpha_1$ and pNMT and to Drs. Mario Rebecchi, Andrew Morris, and Stuart McLaughlin (SUNY at Stony Brook) for their careful reading of the manuscript and helpful discussions.

REFERENCES

1. Neer, E. J. (1994) *Protein Sci. 3*, 3−14.
2. Clapham, D. E., and Neer, E. J. (1997) *Annu. Rev. Pharmacol. Toxicol. 37*, 167−203.
3. Morris, A. J., and Scarlata, S. (1997) *Biochem. Pharmacol. 54*, 429−435.
4. Vaughan, M. (1998) *J. Biol. Chem. 273*, 667−668.
5. Hamm, H. (1998) *J. Biol. Chem. 273*, 669−672.
6. Berman, D., and Gilman, A. G. (1998) *J. Biol. Chem. 273*, 1269−1272.
7. Iyengar, R. (1997) *Science 275*, 42−43.
8. Doupnik, C. A., Davidson, N., Lester, H. A., and Kofuji, P. (1997) *Proc. Natl. Acad. Sci. U.S.A. 94*, 10461−10466.
9. Exton, J. H. (1994) *Annu. Rev. Physiol. 56*, 349−369.
10. Rhee, S. G., and Bae, Y. S. (1997) *J. Biol. Chem. 272* (24), 15045−15048.
11. Boyer, J. L., Graber, S. G., Waldo, G. L., Harden, T. K., and Garrison, J. C. (1994) *J. Biol. Chem. 269* (4), 2814−2819.
12. Ueda, N., Iniguez-Lluhi, J. A., Lee, E., Smrcka, A. V., Robishaw, J. D., and Gilman, A. G. (1994) *J. Biol. Chem. 269*, 4388−4395.
13. Park, D., Hhon, D.-Y., Lee, C.-W., Ryu, S. H., and Rhee, S. G. (1993) *J. Biol. Chem. 268* (5), 3710−3714.
14. Smrcka, A. V., and Sternweis, P. C. (1993) *J. Biol. Chem. 268* (13), 9667−9674.
15. Runnels, L. W., Jenco, J., Morris, A., and Scarlata, S. (1996) *Biochemistry 35*, 16824−16832.
16. Sternweis, P. C., and Robishaw, J. D. (1984) *J. Biol. Chem. 259* (22), 13806−13813.
17. Lee, C. W., Lee, K. H., Lee, S. B., Park, D., and Rhee, S. G. (1994) *J. Biol. Chem. 269* (41), 25335−25338.
18. Hope, M. J., Bally, M. B., Webb, G., and Cullis, P. (1985) *Biochim. Biophys. Acta 812*, 55−65.
19. Cifuentes, M. E., Delaney, T., and Rebecchi, M. J. (1994) *J. Biol. Chem. 269*, 1945−1948.
20. Bartlett, G. R. (1959) *J. Biol. Chem. 234*, 466−468.
21. Romoser, V., Ball, R., and Smrcka, A. V. (1996) *J. Biol. Chem. 271* (41), 25071−25078.
22. Kelly, L. A., Trunk, J. G., Polewski, K., and Sutherland, J. C. (1995) *Rev. Sci. Instrum. 66* (2), 1496−1498.
23. McClosky, M., and Poo, M.-m. (1986) *J. Cell Biol. 102*, 88−96.

24. Jacobson, K., Sheets, E. D., and Simon, R. (1995) *Science 268*, 1441−1442.
25. Berg, O. G., Yu, B.-Z., Rogers, J. and Jain, M. K. (1991) *Biochemistry 30*, 7283−7297.
26. Grasberger, B., Minton, A., DeLisi, C and Metzer, H. (1986) *Proc. Natl. Acad. Sci. U.S.A. 83*, 6258−6262.
27. Gennis, R. B. 1989 *Biomembranes: Molecular Structure and Function* (Cantor, C. R., Ed.) Springer Advanced Texts in Chemistry, Springer-Verlag, New York.
28. Pingoud, A., Boehme, D., Riesner, D., Kownatzki, R., and Maas, G. (1975) *Eur. J. Biochem. 56*, 617−622.
29. Schreiber, G., and Fersht, A. R. (1993) *Biochemistry 32*, 5145−5150.
30. Fersht, A. (1977) *Enzyme Structure and Mechanism*, pp 153−164, Reading, San Francisco, CA.
31. Wenk, M. R., Alt, T., Seelig, A., and Seelig, J. (1997) *Biophys. J. 72*(4), 1719−1731.
32. Cifuentes, M. E., Honkanen, L., and Rebecchi, M. J. (1993) *J. Biol. Chem. 268* (16), 11586−11593.
33. Blank, J. L., Brattain, K. A., and Exton, J. H. (1992) *J. Biol. Chem. 267*, 23069−23075.
34. Boyer, J. L., Waldo, G. L., and T. K., H. (1992) *J. Biol. Chem. 267*, 25451−25456.
35. Camps, M., Carozzi, A., Schnabel, P., Scheer, A., Parker, P. J., and Gierschik, P. (1992) *Nature 360*, 684−686.
36. Camps, M., C., H., Sidiropoulos, D., Stock, J. B., Jakobs, K. H., and Giershik, P. (1992) *Eur. J. Biochem. 206*, 821−831.
37. Katz, A., Wu, D. Q., and Simon, M. I. (1992) *Nature 360*, 686−689.
38. Park, D., Jhon, D., C., L., Lee, K., and Rhee, S. G. 1993 *J. Biol. Chem. 268* (7), 4573−4576.
39. Wu, D., Katz, A., and Simon, M. I. (1993) *Proc. Natl. Acad. Sci. U.S.A. 90*, 5297−5301.
40. Gierschik, P., and Camps, M. (1994) *Methods Enzymol. 238*, 181−195.
41. Paterson, A., Boyer, J. L., Watts, V. J., Morris, A. J., Price, E. M., and Harden, T. K. (1995) *Cell. Signalling 7* (7), 709−720.
42. van der Meer, W., Coker G. and Chen, S. S.-Y. (1994) *Resonance Energy Transfer, Theory and Data*, VCH Publishers, New York.
43. Essen, L., Perisic, O., Cheung, R., Katan, M., and Williams, R. L. (1996) *Nature 380* (18), 595−602.
44. Wall, M. A., Coleman, D. E., Lee, E., Iniguez-Lluhi, J. A., Posner, B. A., Gilman, A. G., and Sprang, S. R. (1995) *Cell 83*, 1047−1058.
45. Sondek, J., Bohm, A., Lambright, D. G., Hamm, H. E., and Sigler, P. B. (1996) *Nature 379*, 369−374.
46. Gardiner, W. C. (1972) *Rates and Mechanims of Chemical Reactions*, W. A. Benjamin, Inc., Reading, MA.
47. Briggs, J. M. (1997) *Biophys. J. 72*, 1915−1916.
48. Haugh, J. M., and Lauffenburger, D. A. (1997) *Biophys. J. 72*, 2014−2031.
49. Neubig, R., Connolly, M. and Remmers, A. (1994) *FEBS Lett. 355*, 251−253.
50. Jenco, J. M., Becker, K. P., and Morris, A. J. (1997) *Biochem. J. 327*, 431−437.
51. Doupnik, C. A., Dessauer, C. W., Slepak, V. Z., Gilman, A. G., Davidson, N., and Lester, H. A. (1996) *Neuropharmacology 35* (7), 923−31.
52. Snyderman, R., Perianin, A., Evans, T., Polakis, P., and Didsbury, J. (1990) in *ADP−Ribosylating Toxins and G Proteins: Insights into Signal Transduction* (Moss, J., and Vaughan, M., Eds.) pp 295−324, American Society for Microbiology, Washington, DC.
53. Zhang, S., Coso, O., Collins, R., Gutkind, J. S. and Simonds, W. F. (1996) *J. Biol. Chem. 271*, 20208−20212.
54. Druey, K. M., et al. (1996) *Nature 379*, 742−745.
55. Doupnik, D. A., Dessauer, C. W., Slepak, C. A., Gilman, A. G., Davidson, N. and Lester, N. A. (1996) *Neurophysiology 7*, 923−931.

BI9811258